Composite Boson Mapping for Lattice Boson Systems

Daniel Huerga,[1] Jorge Dukelsky,[1] and Gustavo E. Scuseria[2]

[1]*Instituto de Estructura de la Materia, C.S.I.C., Serrano 123, E-28006 Madrid, Spain*

[2]*Department of Chemistry and Department of Physics and Astronomy, Rice University, Houston, Texas 77005, USA*

(Received 21 February 2013; revised manuscript received 25 April 2013; published 23 July 2013)

We present a canonical mapping transforming physical boson operators into quadratic products of cluster composite bosons that preserves matrix elements of operators when a physical constraint is enforced. We map the 2D lattice Bose-Hubbard Hamiltonian into 2×2 composite bosons and solve it within a generalized Hartree-Bogoliubov approximation. The resulting Mott insulator-superfluid phase diagram reproduces well quantum Monte Carlo results. The Higgs boson behavior in the superfluid phase along the unit density line is unraveled and in remarkable agreement with experiments. Results for the properties of the ground and excited states are competitive with other state-of-the-art approaches, but at a fraction of their computational cost. The composite boson mapping here introduced can be readily applied to frustrated many-body systems where most methodologies face significant hurdles.

DOI: 10.1103/PhysRevLett.111.045701 PACS numbers: 67.85.Hj, 64.70.Tg, 67.85.Bc, 67.85.De

Introduction.—In the past few years, there has been great experimental progress on the control and manipulation of cold atomic gases loaded in optical lattices, leading to quantum simulators of the Bose-Hubbard model and its Mott insulator to superfluid transition [1]. A notable recent experiment has revealed the Higgs boson behavior across this transition in a 2D optical lattice [2]. There is currently great interest in cold atomic physics for engineering synthetic gauge fields that induce topological phases and phase transitions. This can be accomplished using a combination of laser-induced tunneling with superlattice techniques [3], or by time-periodic shaking of the lattice [4]. From the theoretical perspective, traditional mean-field approaches can describe the phase diagram of bosonic atoms in lattices of various geometries, but only qualitatively [5,6]. Quantum Monte Carlo (QMC) calculations yield a highly accurate description of ground state properties at zero and finite temperatures whenever the system has no frustration [7,8]. Static and dynamic properties have also been studied with the variational cluster approximation (VCA) [9,10]. Extensions of static mean-field approaches involving the use of clusters have been considered [11–13]. In this work, we introduce a theory that maps cluster subspaces of the original Fock space onto composite bosons containing the exact internal dynamics of the cluster, and whose interactions account for residual correlations between the clusters. Because the mapping is canonical, it is then possible to apply standard many-body techniques to this composite boson (CB) Hamiltonian. In this sense, the method builds upon previous slave-particle theories, extending its realm to clusters along the lines of hierarchical mean field theory for quantum magnetism [14]. It could also be considered as an extension to clusters of the on-site slave-boson mapping of the Bose-Hubbard model proposed in Ref. [15]. These ideas are here generalized to interacting bosons systems loaded in optical lattices. We refer to the resulting method as composite boson mean field theory (CBMFT). We demonstrate that the inclusion of higher order fluctuation terms in the composite mean-field approach yields very accurate results. The CB approach to the Bose-Hubbard model unravels the Higgs boson behavior along the particle-hole (p-h) symmetry line and yields remarkable agreement with experimental data [2].

Composite boson mapping.—Let us start our derivation by decomposing the original lattice into a perfect tiled cluster lattice (superlattice). The cluster states are represented by CBs labeled by a position R in the superlattice and by a set of internal quantum numbers α which constitute a complete and orthonormal basis in the Fock space of the cluster. We propose a quadratic mapping of the boson creation (annihilation) operators $a_i^\dagger$ (a_i) in terms of these CBs $b_{R\alpha}^\dagger$ ($b_{R\alpha}$) as

$$a_i^\dagger = \sum_{\alpha\beta} \langle R\alpha | a_i^\dagger | R\beta \rangle b_{R\alpha}^\dagger b_{R\beta}, \quad a_i = (a_i^\dagger)^\dagger, \quad i \in R. \tag{1}$$

Let us now explore the conditions which should be fulfilled by transformation (1) in order to preserve the canonical bosonic commutation relations $[a_i, a_j^\dagger] = \delta_{ij}$. For $i, j \in R$, we insert the transformation in the commutator and obtain

$$[a_i, a_j^\dagger] = \sum_{\alpha\beta\beta'} (\langle R\alpha | a_i | R\beta \rangle \langle R\beta | a_j^\dagger | R\beta' \rangle - \langle R\alpha | a_j^\dagger | R\beta \rangle \langle R\beta | a_i | R\beta' \rangle) b_{R\alpha}^\dagger b_{R\beta'}. \tag{2}$$

The satisfaction of the canonical commutation relations relies on (i) resolution of the identity $\sum_\beta |R\beta\rangle\langle R\beta| = I$, and (ii) fulfillment of the physical constraint $\sum_\alpha b_{R\alpha}^\dagger b_{R\alpha} = I$. The latter condition defines the physical subspace of the CB Fock space, which has a one to one correspondence with the original Fock cluster space. Alternatively, if

$i \in R$ and $j \in R'$ the commutation relation is trivially satisfied due to the commutation of the CBs $[b_{R\alpha}, b^\dagger_{R'\beta}] = \delta_{RR'}\delta_{\alpha\beta}$.

A direct consequence of the CB mapping is that any operator $\hat{O}_R$ that is an algebraic function of the physical bosons (a_i, $a^\dagger_j$) within a single cluster at position R will be mapped to a one-body CB operator $\hat{O}_R = \sum_{\alpha\beta}\langle R\alpha|\hat{O}_R|R\beta\rangle b^\dagger_{R\alpha}b_{R\beta}$. This means that the operator $\hat{O}_R$ changes a cluster configuration α into another cluster configuration β. A formal derivation starting from the mapping (1) in the cluster and using conditions (i) and (ii) is given in the Supplemental Material [16]. In the same way, any product of operators belonging to N different clusters will be mapped to an N-body operator. For the sake of simplicity, we will here restrict ourselves to a density-density interaction that leads to a two-body CB Hamiltonian, since each density operator is contained in a single cluster

$$H = \sum_{ij}[t_{ij}a^\dagger_i a_j + V_{ij}n_i n_j], \qquad n_i = a^\dagger_i a_i. \tag{3}$$

This class of Hamiltonians, with long-range hopping and interactions, covers most of the physical lattice boson models.

We assume a square lattice partitioned into a set of M clusters, each one at position R of a CB superlattice and containing $L \times L$ sites. Next, we formally map the Hamiltonian using the prescription described above and rewrite it in terms of CBs labeled by the occupation configuration of each cluster $\mathbf{n} \equiv \{n_1, \ldots, n_L, \ldots n_{L^2}\}$

$$H_{\mathrm{CB}} = \sum_{R\mathbf{nm}}\langle R\mathbf{n}|H|R\mathbf{m}\rangle b^\dagger_{R\mathbf{n}}b_{R\mathbf{m}} + \sum_{RR'}\sum_{\mathbf{nn'mm'}}\langle R\mathbf{n}R'\mathbf{n}'|H|R\mathbf{m}R'\mathbf{m}'\rangle b^\dagger_{R\mathbf{n}}b^\dagger_{R'\mathbf{n}'}b_{R\mathbf{m}}b_{R'\mathbf{m}'}. \tag{4}$$

For reasons that will become clear below, we will perform a generic unitary transformation among the CBs $b^\dagger_{R\alpha} = \sum_{\mathbf{n}} U^\alpha_{R\mathbf{n}} b^\dagger_{R\mathbf{n}}$. In this new basis, the Hamiltonian can be written as

$$H_{\mathrm{CB}} = \sum_R\sum_{\alpha\beta} T^\alpha_\beta(R) b^\dagger_{R\alpha}b_{R\beta} + \sum_{RR'}\sum_{\alpha\alpha'\beta\beta'} W^{\alpha\alpha'}_{\beta\beta'}(R,R') b^\dagger_{R\alpha}b^\dagger_{R'\alpha'}b_{R\beta}b_{R'\beta'}, \tag{5}$$

where the intracluster $T^\alpha_\beta(R)$ and the intercluster $W^{\alpha\alpha'}_{\beta\beta'}(R,R')$ matrix elements expressed in the transformed basis encode all the information of the original Hamiltonian. The CB Hamiltonian (5) is an exact image of the original boson Hamiltonian provided that the physical constraint in each cluster $\sum_\alpha b^\dagger_{R\alpha}b_{R\alpha} = I$ is satisfied. Furthermore, treating this Hamiltonian by means of standard many-body techniques, we immediately incorporate quantum correlations inside the cluster in an exact way.

Composite boson mean-field theory.—We here treat the CB Hamiltonian in the Hartree-Bogoliubov approximation. In order to proceed further, we have to specify the matrix elements of the initial lattice Hamiltonian. As a first test of CBMFT, we benchmark the Bose-Hubbard Hamiltonian in a 2D square lattice. Namely, $t_{ij} = -t\delta_{i,j+\mathbf{e}}$ where $\mathbf{e}$ is the unit vector in the lattice directions $\mathbf{x}$, $\mathbf{y}$, and $V_{ij} = V\delta_{i,j}$ is the on-site Hubbard repulsion. In what follows, we omit V and measure all quantities in units of V. Assuming a uniform 2D lattice with translational symmetry, we first perform a Fourier transform of the CB boson operators $b^\dagger_{\mathbf{R}\alpha} = (1/\sqrt{M})\sum_{\mathbf{k}} e^{-iL\mathbf{k}\cdot\mathbf{R}} b^\dagger_{\mathbf{k}\alpha}$, leading to

$$H_{\mathrm{CB}} = \sum_{\alpha\beta} T^\alpha_\beta \sum_{\mathbf{k}} b^\dagger_{\mathbf{k}\alpha}b_{\mathbf{k}\beta} + \frac{1}{M}\sum_{\alpha\alpha'\beta\beta'} W^{\alpha\alpha'}_{\beta\beta'} \sum_{\mathbf{k}_1\mathbf{k}_2\mathbf{q}} \gamma_{\mathbf{q}} b^\dagger_{\mathbf{k}_1\alpha}b^\dagger_{\mathbf{k}_2+\mathbf{q}\alpha'}b_{\mathbf{k}_1+\mathbf{q}\beta}b_{\mathbf{k}_2\beta'}, \tag{6}$$

where we have introduced $\gamma_{\mathbf{q}} = \cos(Lq_x) + \cos(Lq_y)$ after a symmetrization of the two-body matrix elements $W^{\alpha\alpha'}_{\beta\beta'}$ in order to preserve the lattice C_4 symmetry. Details on the calculation of these matrix elements can be found in the Supplemental Material [16]. Next, we assume a condensation of the CBs in the $\mathbf{k} = \mathbf{0}$, $\alpha = 0$ state by introducing a shift transformation $b_{\mathbf{k}=\mathbf{0},\alpha=0} = b^\dagger_{\mathbf{k}=\mathbf{0},\alpha=0} = \sigma\sqrt{M}$. This transformation manifestly violates the physical constraint as it induces mixtures with unphysical states. This is a common problem to all slave-particle theories treated in a mean-field approach. However, this mixture is expected to be less severe with increasing cluster sizes, such that in the limit of very large clusters it must be negligible. Thus, we relax it and impose a global constraint on the CB density, $\sum_R\sum_\alpha b^\dagger_{R\alpha}b_{R\alpha} = M$. Transforming to momentum space and shifting, this global physical constraint becomes

$$\sigma^2 + \frac{1}{M}\sum_{\alpha\neq 0}\sum_{\mathbf{k}} b^\dagger_{\mathbf{k}\alpha}b_{\mathbf{k}\alpha} = 1, \tag{7}$$

where we have neglected the fluctuations of the condensed $\alpha = 0$ CB. Equation (7) defines σ^2 as the CB condensate fraction. Inserting the constraint (7) by means of a Lagrange multiplier λ in the CB Hamiltonian (6) and applying a mean-field decoupling, we arrive to a quadratic Hamiltonian of the form

$$H_{\mathrm{MF}} = H^{(0)} + \sum_{\mathbf{k}}\sum_{\alpha\neq 0,\beta\neq 0} A_{\mathbf{k}\alpha\beta}b^\dagger_{\mathbf{k}\alpha}b_{\mathbf{k}\beta} + \sum_{\mathbf{k}}\sum_{\alpha\neq 0,\beta\neq 0}(B_{\mathbf{k}\alpha\beta}b^\dagger_{\mathbf{k}\alpha}b^\dagger_{-\mathbf{k}\beta} + B_{\mathbf{k}\alpha\beta}b_{-\mathbf{k}\beta}b_{\mathbf{k}\alpha}). \tag{8}$$

The specific form of $H^{(0)}$ and the matrices $A_{\mathbf{k}\alpha\beta}$ and $B_{\mathbf{k}\alpha\beta}$ can be found in the Supplemental Material [16].

The quadratic mean-field Hamiltonian (8) can be diagonalized by means of a Bogoliubov transformation $c^\dagger_{\mathbf{k}\alpha} = \sum_\beta X_{\mathbf{k}\beta\alpha} b^\dagger_{\mathbf{k}\beta} - \sum_\beta Y_{\mathbf{k}\beta\alpha} b_{-\mathbf{k}\beta}$ leading to the Bogoliubov eigensystem equation [17]

$$\begin{pmatrix} A_{\mathbf{k}} & 2B_{\mathbf{k}} \\ -2B^*_{\mathbf{k}} & -A^*_{\mathbf{k}} \end{pmatrix} \begin{pmatrix} X_{\mathbf{k}} \\ Y_{\mathbf{k}} \end{pmatrix} = \omega_{\mathbf{k}} \begin{pmatrix} X_{\mathbf{k}} \\ Y_{\mathbf{k}} \end{pmatrix}, \tag{9}$$

where the positive eigenvalues $\omega_{\mathbf{k}}$ determine the excitation spectrum. The Bogoliubov equation depends on the generic transformation U previously defined. Upon minimization of the free energy with respect to the condensed CB structure $U^0_{\mathbf{m}}$ we derive a Hartree-like equation for this transformation. The resulting equation can be cast in matrix form

$$\sum_{\mathbf{n}} h_{\mathbf{m},\mathbf{n}} U^0_{\mathbf{n}} = \lambda U^0_{\mathbf{m}}. \tag{10}$$

The derivation of the matrix elements of h for $L \times L$ clusters, given in the Supplemental Material [16], is straightforward though lengthy. The Hartree Hamiltonian h depends on the unitary transformation U, on the Bogoliubov amplitudes $X_{\mathbf{k}}$, $Y_{\mathbf{k}}$, and on the fraction of the condensate σ^2. Strictly speaking, the self-consistent Hartree diagonalization provides a single eigenvector defining the structure of the condensed CB and the corresponding lowest eigenvalue, which is the Lagrange multiplier λ. However, after attaining self-consistency the matrix diagonalization procedure supplies a complete set of eigenstates that are orthogonal to the condensed CB. It is in this basis orthogonal to the condensate where the mean-field Hamiltonian (8) is expressed. We seek a self-consistent solution of the coupled set of equations given by the Hartree eigensystem (10) which fixes the unitary transformation U and the Langrange multiplier λ, the Bogoliubov equations (9) that provide the Bogoliubov amplitudes $X_{\mathbf{k}}$ and $Y_{\mathbf{k}}$, together with the expectation value of the physical constraint (7) that determines the CB condensed fraction σ^2.

2D Bose-Hubbard model results.—We start with benchmark calculations based on 2×2 clusters describing the first Mott lobe characterized by a fixed density per site $\rho = 1$. Within this phase, the structure of the unitary transformation U and the CB condensed fraction σ^2 are μ independent. The structure of the condensed CB, dictated by U^0, is a linear combination of cluster states with $|\mathbf{n}| = 4$. The relevant CB fluctuations are pairs of particle ($|\mathbf{n}| = 5$) and hole ($|\mathbf{n}| = 3$) cluster states. In addition, particle- and holelike excitation eigenvalues have a linear dependence on the chemical potential for fixed t. Both excitations cross each other at the p-h symmetry line, where the gap is doubly degenerate. The edges of the first Mott lobe are determined by the vanishing of the gap,

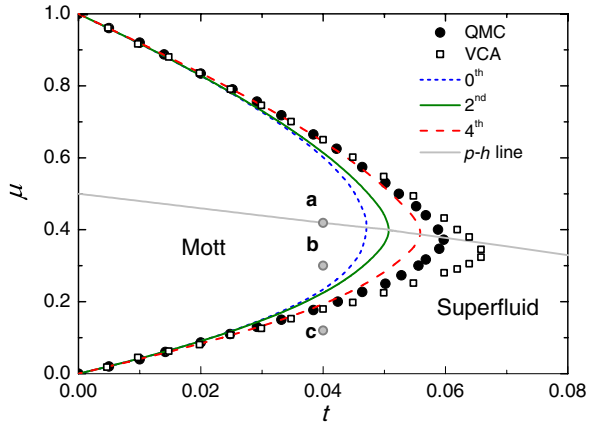

FIG. 1 (color online). Phase diagram of the first lobe of the Mott insulator to superfluid transition. The dotted, solid, and dashed curves show the 2×2 CBMFT results in increasing order of approximation. The p-h symmetry line traverses the Mott lobe and extends into the superfluid region at a constant density $\rho = 1$. Black circles are QMC results from Ref. [7]. Squares display VCA results from Ref. [9]. Gray circles display three points in parameter space for which the dispersions are analyzed in Fig. 3.

indicating the appearance of a Goldstone mode at $\mathbf{k} = \mathbf{0}$ related to the $U(1)$ symmetry breaking in the superfluid.

Figure 1 shows the phase diagram of the Bose-Hubbard model in three different CB mean-field approximations. The zeroth order approximation neglects fluctuations and solves the Hartree equations exclusively. The edges of the Mott lobe are determined in this case by a deviation from the density $\rho = 1$. This zeroth order approximation is equivalent to the cluster mean-field calculations of Refs. [11,13] producing the same phase diagram (dotted line in Fig. 1). The 2nd and 4th order approximations go beyond previous cluster mean-field approximations incorporating fluctuations by means of a self-consistent solution of the Bogoliubov (9) plus Hartree (10) equations linked by

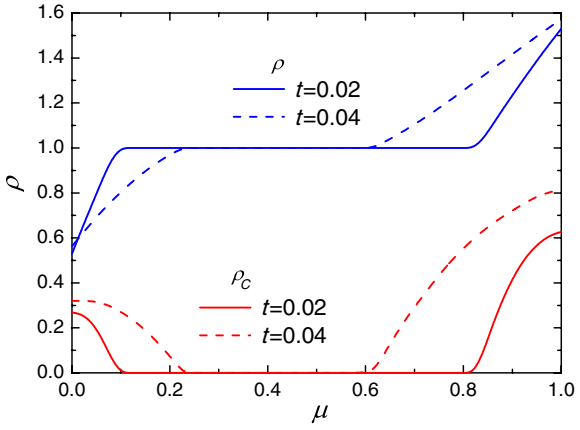

FIG. 2 (color online). Total density (ρ) and condensate density (ρ_c) for $t = 0.02$ (solid line) and $t = 0.04$ (dashed line) within the 2nd order approximation.

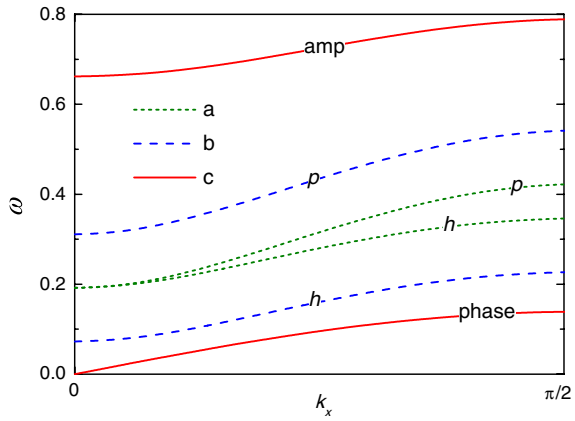

FIG. 3 (color online). Dispersion modes for $t = 0.04$: particle- and holelike excitation modes at (a) the p-h symmetry line ($\mu = 0.419$), and (b) inside the Mott insulator ($\mu = 0.30$), and amplitude- and phase-like modes at (c) in the superfluid ($\mu = 0.12$).

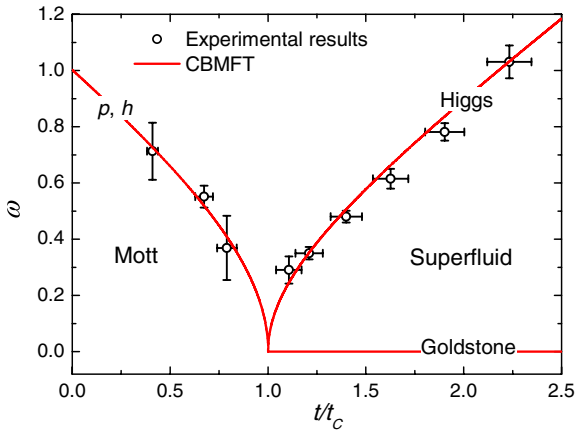

FIG. 4 (color online). Higgs, Goldstone, particle, and hole modes along the p-h symmetry line computed within 2nd order CBMFT (solid line). Experimental data points from Ref. [2].

the physical condition (7). The 2nd order approximation neglects two-body interactions among fluctuating bosons, while the 4th order solves the three coupled equations in full. As the approximation order increases, CBMFT shows clear convergence towards QMC data. VCA results, which were related in Ref. [9] to a linear approximate CB mapping, extend well beyond the QMC Mott lobe. Also shown in Fig. 1 is the extension of the p-h line into the superfluid phase characterized by density $\rho = 1$.

The full self-consistent 4th order approximation does not describe the gapless feature of the superfluid phase correctly. Although ways to correct this deficiency have been suggested [18], in the rest of this Letter we will focus on the 2nd order approximation that strictly preserves the gapless spectrum when $U(1)$ symmetry is broken.

Figure 2 shows the total density $\rho = \langle\phi|a_j^\dagger a_j|\phi\rangle$ and the condensate density $\rho_c = |\langle\phi|a_j^\dagger|\phi\rangle|^2$ for hopping values of $t = 0.02$ and 0.04. The plateau characterizing the Mott phase is reduced for larger t. Outside this region, the superfluid has noncommensurate density. The condensate density of physical bosons, representing the coherence of the superfluid phase, vanishes in the Mott phase. VCA results for $t = 0.02$ [9,10] compare well with our results.

In Fig. 1, we have depicted three characteristic points at $t = 0.04$; namely, point a is at the p-h line in the Mott phase, point b is still in the Mott phase but away from the p-h line, and point c is in the superfluid phase. Figure 3 shows particle- and holelike excitations for $k_y = 0$ as a function of k_x for points a and b inside the Mott phase. The degeneracy of the particle and hole modes for point a approaching $\mathbf{k} = \mathbf{0}$ is clearly seen in this figure. Away from the p-h line and still in the Mott phase (point b), this degeneracy is broken and the hole is favored against the particle mode. Well inside the superfluid phase (point c), we recognize a gapless mode (Goldstone mode) with the characteristic linear dispersion at low momentum, as well as a gapped mode. An analysis of the CB structure $U_{\mathbf{m}}^{\alpha}$ of each mode, similar to the one performed in Ref. [11], shows that the gapless mode is a phaselike mode, while the gapped mode is an amplitude-like mode.

The phase transition taking place at the lobe tip along a constant density line ($\rho = 1$) can be understood in terms of an $O(2)$ relativistic field theory, as has been recently discussed in Refs. [2,19]. Figure 4 displays how doubly degenerate excitations along the p-h line inside the Mott insulator vanish at the critical point. In the superfluid region, one of them remains at zero excitation energy (Goldstone mode) while the other one grows for increasing hopping (Higgs mode). In both cases, their structure mixes particle- and holelike states of the cluster. The CBMFT results not only match the experimental data [2] remarkably well but also gives an excellent description of the critical point.

Conclusions.—We have introduced a cluster composite boson mapping which separates intra- and intercluster degrees of freedom. The former are treated exactly while the latter can be approximated using standard many-body methods applied to the resulting CB Hamiltonian. We have here shown that a mean-field approximation to the CB interaction for the Bose-Hubbard model produces an accurate description of the Mott-superfluid phase diagram compared to QMC results. Densities and dispersions are found in quantitative agreement with more sophisticated techniques like the VCA. The recently measured Higgs mode is also computed and found to be in remarkable agreement with experiment. Further improvement of the theory beyond the mean-field 2nd order approximation employed in this work is feasible. Most importantly, CBMFT is readily applicable to other many-body problems where frustration, synthetic gauge fields, or long-range interactions pose significant hurdles to existing state-of-the-art methodologies.

We acknowledge useful discussions with C. A. Jimenez-Hoyos, L. Isaev, and G. Ortiz. This work was supported by Grants No. FIS2009-07277, No. FIS2012-34479, and No. BES-2010-031607 of the Spanish Ministry of Economy and Competitiveness. G. E. S. is supported by U.S. DOE Award No. DE-FG02-09ER16053 and The Welch Foundation (C-0036).

[1] M. Lewenstein, A. Sanpera, and V. Ahufinger, *Ultracold Atoms in Optical Lattices: Simulating Quantum Many-Body Systems* (Oxford University, New York, 2012).
[2] M. Endres, T. Fukuhara, D. Pekker, M. Cheneau, P. Schauss, C. Gross, E. Demler, S. Kuhr, and I. Bloch, Nature (London) **487**, 454 (2012).
[3] D. Jaksch and P. Zoller, New J. Phys. **5**, 56 (2003).
[4] P. Hauke, O. Tieleman, A. Celi, C. Ölschläger, J. Simonet, J. Struck, M. Weinberg, P. Windpassinger, K. Sengstock, M. Lewenstein, and A. Eckardt, Phys. Rev. Lett. **109**, 145301 (2012).
[5] D. van Oosten, P. van der Straten, and H. T. C. Stoof, Phys. Rev. A **63**, 053601 (2001).
[6] S. D. Huber, E. Altman, H. P. Büchler, and G. Blatter, Phys. Rev. B **75**, 085106 (2007).
[7] B. Capogrosso-Sansone, S. G. Soyler, N. Prokof'ev, and B. Svistunov, Phys. Rev. A **77**, 015602 (2008).
[8] L. Pollet, C. Kollath, K. Van Houcke, and Matthias Troyer, New J. Phys. **10**, 065001 (2008).
[9] M. Knap, E. Arrigoni, and W. von der Linden, Phys. Rev. B **83**, 134507 (2011).
[10] E. Arrigoni, M. Knap, and W. von der Linden, Phys. Rev. B **84**, 014535 (2011).
[11] D. Pekker, B. Wunsch, T. Kitagawa, E. Manousakis, A. S. Sørensen, and E. Demler, Phys. Rev. B **86**, 144527 (2012).
[12] D. Yamamoto, I. Danshita, and C. A. R. Sá de Melo, Phys. Rev. A **85**, 021601 (2012).
[13] T. McIntosh, P. Pisarski, R. J. Gooding, and E. Zaremba, Phys. Rev. A **86**, 013623 (2012).
[14] L. Isaev, G. Ortiz, and J. Dukelsky, Phys. Rev. B **79**, 024409 (2009).
[15] D. B. M. Dickerscheid, D. van Oosten, P. J. H. Denteneer, and H. T. C. Stoof, Phys. Rev. A **68**, 043623 (2003).
[16] See Supplemental Material at http://link.aps.org/supplemental/10.1103/PhysRevLett.111.045701 for additional details about the composite boson mapping.
[17] J. P. Blaizot and G. Ripka, *Quantum Theory of Finite Systems* (MIT, Cambridge, MA, 1986).
[18] V. I. Yukalov, Phys. Part. Nucl. **42**, 460 (2011).
[19] L. Pollet and N. Prokof'ev, Phys. Rev. Lett. **109**, 010401 (2012).